

RESEARCH PAPER

Sustainable Biodiesel Production from Edible Oil through Transesterification with Waste Iron-Based α -Fe₂O₃/SiO₂ Heterogeneous Catalyst: Performance and Reusability Studies

Faezeh Mosalmanzadeh, Tara Ghaffarinejad, Ramin Karimzadeh*

Faculty of Chemical Engineering, Tarbiat Modares University (TMU), Jalal Al Ahmad Highway, P .O. Box 14155-4838, Tehran, Iran

ARTICLE INFO

Article History:

Received 29 July 2025

Revised 9 September 2025

Accepted 14 December 2025

Keywords:

Iron waste, heterogeneous catalyst, α -Fe₂O₃/SiO₂, transesterification, biodiesel, thermal activation, renewable energy.

ABSTRACT

The development of innovative and sustainable processes for biodiesel production, as one of the most important renewable biofuels, plays a crucial role in reducing dependence on fossil fuels and mitigating environmental pollution. Considering the high costs of conventional processes and challenges in designing stable catalysts, the utilization of waste-derived materials for synthesizing heterogeneous catalysts represents a valuable and innovative approach. In this study, an iron-silica catalyst was synthesized using waste iron, and its performance was evaluated in the transesterification reaction for biodiesel production. The results demonstrated that the synthesized catalyst exhibited high activity, stability, and reusability, facilitating biodiesel production with significant yield. Furthermore, FTIR and XRD analyses confirmed the presence of methyl ester groups in the biodiesel and the structural features of the catalyst, highlighting the effectiveness of the proposed synthesis route. These findings suggest that using waste iron for the synthesis not only reduces production costs but also contributes to advancing green and sustainable technologies. Ultimately, this approach may provide a foundation for future research focused on industrial-scale applications and further optimization of operating parameters in sustainable biodiesel production.

How to cite this article

Mosalmanzadeh F, Ghaffarinejad T, Karimzadeh R, Sustainable Biodiesel Production from Edible Oil through Transesterification with Waste Iron-Based α -Fe₂O₃/SiO₂ Heterogeneous Catalyst: Performance and Reusability Studies, Journal of Oil, Gas and Petrochemical Technology. 2025; 12(2): 81-96. DOI:10.22034/jogpt.2026.537855.1142

1. INTRODUCTION

Over the last few decades, biodiesel has attracted considerable attention as a renewable and environmentally friendly alternative to conventional fossil fuels. Biodiesel produced from vegetable oils and animal fats offers advantages such as

biodegradability, renewability, and reduced greenhouse-gas emissions, which makes it a promising option for the sustainable transportation and energy systems [1]. Nevertheless, conventional biodiesel production processes still face several challenges, including high production costs, limited catalyst stability, difficulties in catalyst recovery,

* Corresponding Author: ramin@modares.ac.ir;

and suboptimal conversion efficiency under practical operating conditions [2].

Simultaneously, large volumes of industrial iron-containing wastes—particularly slags and machining residues from steel and mining industries—pose a significant environmental and economic burden because they are often disposed of without valorization ([3],[4]). These wastes, however, frequently possess physicochemical properties that can be harnessed for value-added applications. Converting iron-rich waste into functional materials is therefore an attractive route that addresses both waste management and resource efficiency.

Iron oxides, and hematite ($\alpha\text{-Fe}_2\text{O}_3$) in particular, have desirable attributes for heterogeneous catalysis, including good thermal and chemical stability, low cost, and suitable surface properties for the active site dispersion ([5],[6]). A variety of synthetic routes for $\alpha\text{-Fe}_2\text{O}_3$ nanoparticles have been reported—chemical precipitation, co-precipitation, sol-gel, hydrothermal, sonochemical, and spray pyrolysis—with chemical precipitation being notable for its simplicity, low cost, and controllable particle morphology [7]. Standard characterization techniques such as X-ray diffraction (XRD) and Fourier-transform infrared spectroscopy (FTIR) are routinely used to confirm phase purity and identify Fe–O bonding and functional groups in both catalysts and reaction products [8]. In biodiesel synthesis, process parameters—including the methanol-to-oil molar ratio, catalyst loading, and reaction temperature—critically influence conversion and selectivity and therefore require careful optimization ([9],[10],[11]). Silica supports (SiO_2) are widely used to stabilize and disperse active iron species because of their high surface area, thermal stability, and chemical inertness [12].

Recent literature shows significant progress in Fe-based and Fe/ SiO_2 -derived catalysts for biodiesel production. For example, Hanif et al., (2024) synthesized nano-magnetic $\text{CaO/Fe}_2\text{O}_3/\text{feldspar}$ catalysts and reported high biodiesel yields from waste oils [13]. Rahimi et al., (2021) developed

$\text{MgO/Fe}_2\text{O}_3\text{-SiO}_2$ core-shell magnetic nanocatalysts and employed response surface methodology (RSM-CCD) to optimize reaction conditions and achieving enhanced conversion efficiencies [14]. Ziyadi et al., (2020) prepared $\text{Fe}_2\text{O}_3@\text{SiO}_2\text{-SO}_3\text{H}$ nanofibers that exhibited strong acidic activity and high catalytic performance in esterification/transesterification reactions [15]. Teo et al., (2022) reported $\text{CaSO}_4/\text{Fe}_2\text{O}_3\text{-SiO}_2$ core-shell nanoparticles that improved transesterification kinetics and product quality [16]. Ursachi et al., (2019) synthesized magnetic $\alpha\text{-Fe}_2\text{O}_3/\text{MCM-41}$ nanocomposites and demonstrated improved structural properties and catalytic activity in model reactions [17]. While these studies confirm the potential of iron-based nanostructures for biodiesel applications, many rely on carefully prepared synthetic precursors or costly reagents, and few systematically explore the direct valorization of industrial iron waste as a precursor for the catalytic materials.

Accordingly, a clear knowledge gap remains: despite advances in iron-based catalysts, the direct use of industrial iron waste as a low-cost, sustainable precursor for synthesizing $\alpha\text{-Fe}_2\text{O}_3/\text{SiO}_2$ heterogeneous catalysts—combined with comprehensive optimization and recyclability assessment under relevant transesterification conditions—has not been sufficiently investigated. Addressing this gap can simultaneously reduce feedstock costs, improve process sustainability, and provide an effective pathway for the industrial waste valorization.

The present study aims to fill this gap by (i) synthesizing an $\alpha\text{-Fe}_2\text{O}_3/\text{SiO}_2$ nanocomposite catalyst using industrial iron waste as the iron source, (ii) characterizing the catalyst by XRD, FTIR, and other physico-chemical techniques, (iii) evaluating the catalyst's activity, selectivity, and reusability in the transesterification of refined edible oil to biodiesel, and (iv) optimizing key operational parameters to maximize biodiesel yield and process robustness. The resulting data are intended to clarify the feasibility of converting iron waste into effective heterogeneous catalysts and to inform further

Table 1. Specifications and sources of materials used

Material	Formula	Grade	Source
Sulfuric acid	H ₂ SO ₄	98%	Merck, Germany
Distilled water	H ₂ O	-	Laboratory supply
Iron flakes	Fe	Industrial	-
Silica	SiO ₂	-	-
Hydrogen peroxide	H ₂ O ₂	30% w/w	Mojallali Chemical Co.
Sunflower oil	-	Edible grade	Ladan brand
Methanol	CH ₃ OH	Industrial	Kimia Exir, Iran
Zeolite A4	-	Industrial	Sigma-Aldrich

scale-up and techno-economic assessment.

2. Experimental section Material and Method

2.1. Materials

All chemicals and reagents used in this study were of commercial/industrial grade and were used without further purification. The specifications and sources of materials are provided in Table 1.

2.2. Method

2.2.1. Synthesis of Catalyst Process (α -Fe₂O₃/SiO₂)

2.2.1.1. Synthesis of Iron(II) Sulfate Precursor

The first step of the catalyst synthesis was the

preparation of an iron(II) sulfate (FeSO₄·nH₂O) precursor through the reaction between sulfuric acid and iron waste. A weighed amount of iron flakes (1 g) was added to 40% sulfuric acid in a glass reactor under constant stirring. The reaction was conducted at three temperatures (60 °C, 70 °C, and 80 °C) and for varied time periods (8, 9, 10, and 11 hours) to determine the optimum dissolution conditions.

The suspension was filtered after reaction to eliminate unreacted solids and insoluble impurities. The iron sulfate yield was determined based on the mass of iron dissolved compared to the initial amount using the following equation:

$$Yield (\%) = \frac{\text{Initial mass of Fe} - \text{Final residual mass}}{\text{Initial mass of Fe}} \times 100 \quad (1)$$

The parameter ranges used in the study are summarized in Table 2.

Table 2. Experimental parameters for Iron dissolution in sulfuric acid

Parameter	Range/Amount
Sulfuric acid concentration	40%
Amount of iron scrap	1 g
Temperature	60°C,70°C,80°C
Reaction time	8 h,9 h,10 h,11h

2.2.1.2. Deposition of Iron Species onto Silica

Silica (1g) was mixed with the iron(II) sulfate solution from the first step. The slurry was then stirred at room temperature for 1 hour to achieve a homogeneous distribution of the iron species on the silica surface.

Then, 30 g of 10% hydrogen peroxide (H₂O₂) solution was slowly dropwise added as an oxidizing agent to catalyze Fe²⁺ to Fe³⁺ oxidation and facilitate the creation of iron oxide. The suspension was further stirred for another 2 hours at room temperature, prior to aging for 12 hours under no disturbance. Following aging, the resultant solid product was filtered and washed several times with deionized water to eliminate residual salts and unreacted species [5].

2.2.1.3. The drying of catalyst and its thermal activation

The solid was dried in an oven at 100 °C for 6 hours to remove water by evaporation ([18],[19]). This was followed by calcination in a muffle furnace at 700 °C for 2 hours for the crystallization of the hematite (α-Fe₂O₃) phase and to firmly anchor it onto the silica matrix [20]. The obtained catalyst was stored in a desiccator to prevent moisture absorption prior to characterization and catalytic testing.

Techniques such as FTIR and XRD were employed to establish the chemical structure and crystalline phase of the α-Fe₂O₃/SiO₂ catalyst produced [8]. The conditions used in this step are presented in Table 3.

2.2.2. Procedure for Biodiesel Production

To prepare the biodiesel, 14 g of sunflower

refined oil dried in an oven at 110 °C for 6 hours in advance was mixed with anhydrous methanol. Methanol was pre-dried in advance using zeolite A4 for 12 hours to eliminate trace water and to prevent hydrolysis reaction [21].

The α-Fe₂O₃/SiO₂ prepared catalyst was added to the reaction mixture, and the transesterification reaction was carried out under controlled heating using a magnetic stirrer. The reaction was carried out for a fixed time of 6 hours for varied experimental conditions to determine optimum performance parameters .

The variables studied were:

Methanol-to-oil molar ratio: 8:1, 10:1, 12:1, and 14:1

Catalyst loading (wt% of oil): 0.05 wt%, 0.07 wt%, and 0.10 wt%

Reaction temperature: 50 °C, 60 °C, and 70 °C

Following each reaction, the reaction mixture was centrifuged to enable phase separation. The resulting product was then placed in a decanter. Due to the differences in density, two different layers were produced: an upper clearer, lighter layer consisting of biodiesel, and a darker, denser lower layer consisting of glycerol.

The biodiesel layer was decanted, and it was washed 2–3 times with distilled water until the aqueous layer became clear. The biodiesel was dried in an oven at 60 °C for 6 hours to remove methanol and water.

Biodiesel yield was calculated using the formula:

$$\text{Biodiesel Yield (\%)} = \frac{\text{Mass of purified biodiesel}}{\text{Mass of oil used}} \times 100 \quad (2)$$

Table 3. Catalyst composition and thermal treatment parameters

Silica (g)	H ₂ O ₂ Concentration (%)	H ₂ O ₂ Amount (g)	Aging (h) Time	Oven time (h)	Oven temp (°C)	Furnace Temp (°C)	furnace time (h)
1	10	30	12	6	100	700	2

To measure the physical properties of the biodiesel formed, the density and kinematic viscosity of the biodiesel were measured. The product biodiesel was 0.73 g/cm³ density and 4.3 mm²/s viscosity, which meet the biodiesel fuel acceptable limit.

Further product quality analysis and catalyst activity were analyzed using FTIR in which proximate chemical composition and molecular structure analysis were performed. The biodiesel production test parameters are summarized in Table 4.

Table 4. Biodiesel production test parameters

Parameter	Design	Operational
Temperature (°C)	51.5	59.47
Pressure (kPa)	7171	7584
Flow rate (kg/hr)	450300	360070

the iron dissolution in 40% sulfuric acid was examined under three levels of temperature (60 °C, 70 °C, and 80 °C) and four time periods (8, 9, 10, and 11 hours). The result of the parametric study is given in Table 5.

Table 5. Effect of reaction time and temperature on dissolution efficiency

Absorber column	Simulation temperature (°C)	Operational temperature (°C)	Error %
Tray No. 5	62.7	62.12	+0.009
Tray No. 10	67.63	65.22	-0.031
Tray No. 15	74.93	73.78	+1.56
Tray No. 20	82.16	80.50	+2.06

These observations are consistent with previous studies reporting that elevated temperatures (71–110 °C) increase the solubility of iron in sulfuric acid [7]. However, very high temperatures may accelerate energy consumption and promote side reactions or structural degradation of the catalyst. Therefore, selecting 80 °C and 11 h represents a practical compromise, achieving high conversion without compromising catalyst integrity.

From an industrial perspective, maintaining a moderate reaction temperature also reduces energy requirements and improves process feasibility.

3.2. Catalyst activation

Journal of Oil, Gas and Petrochemical Technology 2025(12): 81-96, Summer and Autumn 2025



3. Results and Discussion

3.1. Synthesis of α -Fe₂O₃/SiO₂ Catalyst

The α -Fe₂O₃/SiO₂ catalyst was successfully synthesized through a multi-step procedure involving the dissolution of iron waste in sulfuric acid, deposition onto a silica support, and subsequent thermal treatment. The optimization of synthesis conditions, including reaction temperature and time, was essential to achieve maximum iron dissolution efficiency and catalytic activity.

To determine the best operating conditions,

As shown in Table 5, both temperature and reaction time significantly influenced the iron dissolution rate. At 60 °C, increasing the reaction time from 8 h to 11 h raised the efficiency from 74% to 89%. Higher temperatures further enhanced the dissolution, reaching 92% at 80 °C for 11 h.

The silica content was kept constant at 1 g in all experiments. The silica was added to the solution and stirred at room temperature for 1 h. Then, 30 g of 10% hydrogen peroxide was added dropwise, and the system underwent an aging process for 12 h [22]. The resulting solid was washed with deionized water, dried at 100 °C for 6 h, and finally calcined at 700 °C for 2 h [23]. FTIR and XRD analyses confirmed the successful formation of the hematite phase (α -Fe₂O₃) well dispersed on the silica support.

3.2.1. X-ray Diffraction (XRD) Analysis

X-ray diffraction (XRD) analysis was employed as one of the principal methods to study the crystalline structure of the prepared iron-based catalyst. The XRD analysis revealed the presence of the hematite phase (α -Fe₂O₃) with a well-ordered structure and excellent crystallinity in the sample. Well-defined diffraction peaks were observed at 2θ positions of approximately 24.1°, 33.1°, 35.6°, 40.8°, 49.4°, 54.0°, 57.5°, and 62.4°, which show excellent consistency with the standard reference pattern of hematite (JCPDS Card No. 33-0664) [10]. These peaks correspond to the (012), (104), (110), (113), (024), (116), (018), and (214) crystal planes, respectively. The narrowness and high intensity of the peaks confirm the formation of a high-purity α -Fe₂O₃ phase with relatively large crystal sizes. The absence of notable peak broadening also confirms

the well-developed, highly ordered crystalline nature of the sample. These characteristics are crucial for catalytic applications since phase purity and ordered structure of the hematite are essential for both redox reactions and overall catalytic activity. Additionally, the high peak intensity of hematite indicates satisfactory interaction between iron species and silica support, which enhances the dispersion of the active phase in the catalyst and improves structural stability. The highly crystalline nature and purity of the structure contribute to a high density of surface active sites, increased contact with reactants, and reduction in the activation energy of the catalytic process. Overall, the XRD analysis demonstrates that the synthesized catalyst possesses a well-defined crystal structure and a single hematite phase, making it a highly suitable candidate for catalytic applications, particularly in biodiesel synthesis.

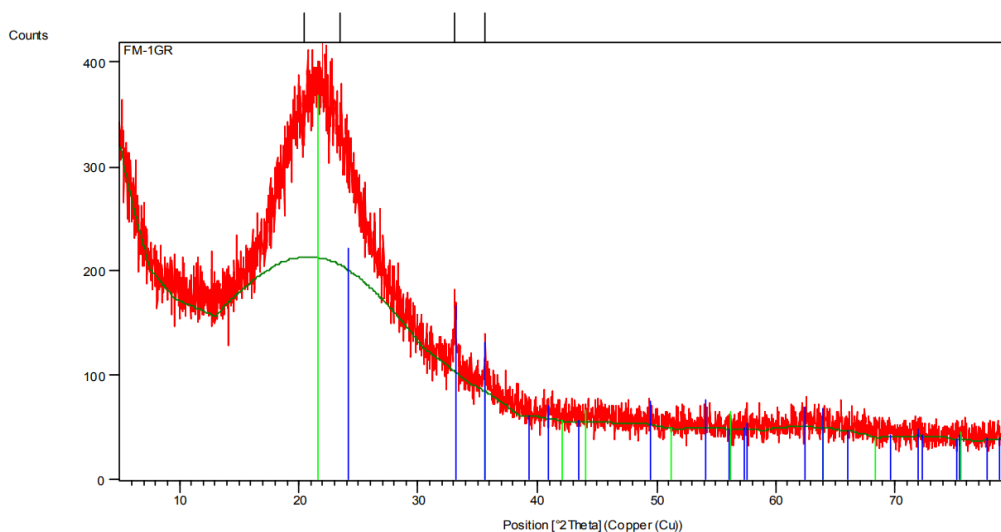


Figure 1. The XRD pattern of α -Fe₂O₃/SiO₂ catalyst

3.2.2. Fourier-Transform Infrared Spectroscopy (FTIR) Analysis

FTIR spectroscopy was employed to investigate the chemical functionalities and the structural features of the powder catalyst synthesized prior to its application in the transesterification reaction. The analysis was designed to confirm the formation and interaction of iron oxide species with the silica support. The strongest seen absorption bands were taken at 535 cm^{-1} and 436 cm^{-1} , corresponding to bending vibrations of Fe–O bonds characteristic for hematite ($\alpha\text{-Fe}_2\text{O}_3$) structures and confirm the presence of iron oxide species in the matrix of the catalyst.

A significant peak at 1122 cm^{-1} was assigned to asymmetric stretching of Si–O–Si, indicating the silica structure [8]. This band also falls in the fingerprint region usually associated with ester

groups, so it can indicate the possibility of residual organosilicon compounds or adsorbed esters resulting from the synthesis reaction. The band at 1594 cm^{-1} , which is related to C=C stretching vibrations, may be due to aromatic frameworks or weakly adsorbed intermediate organic residues on the catalyst surface.

Broad absorptions at 3736 cm^{-1} and 3306 cm^{-1} were attributed to O–H stretching vibrations, pointing toward the presence of surface hydroxyl groups as well as adsorbed water typical features in porous silica materials that can enhance surface reactivity. Overall, the FTIR findings confirm the effective preparation of a silica-supported iron oxide catalyst with relevant surface functionalities expected to be accountable for its catalytic performance in the synthesis of biodiesel.

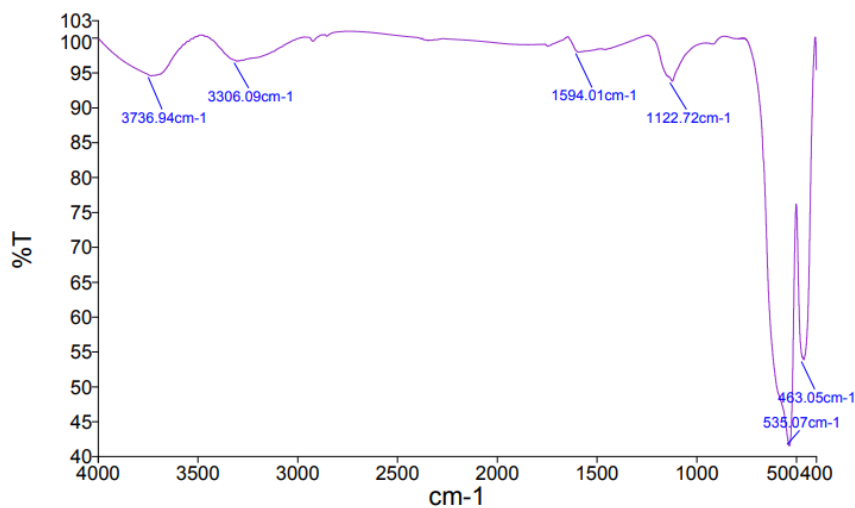


Figure 2. The FTIR spectrum of the produced catalyst

3.3. Biodiesel production

The catalytic performance of the synthesized $\alpha\text{-Fe}_2\text{O}_3/\text{SiO}_2$ nanocomposite was evaluated through a series of transesterification reactions using purified sunflower oil and methanol. The effects of three key variables—methanol-to-oil molar ratio, catalyst loading, and reaction temperature—were systematically investigated to determine the optimum conditions for the maximum biodiesel yield.

3.3.1. Effect of Methanol-to-Oil Molar Ratio

The methanol-to-oil molar ratio has the greatest impact among all the parameters in shifting the transesterification reaction equilibrium towards the products. Four molar ratios of 8:1, 10:1, 12:1, and 14:1 were tested, and the outcomes are presented in Table 6.

As can be seen from Table 5 and Figure 6, increasing the molar ratio of methanol to oil from 8:1 to 12:1 significantly increased the yield of biodiesel, reflecting the excess methanol forward reaction kinetics. However, increasing the ratio further to 14:1 led to a reduction in yield. This is likely due to the reactant dilution and also the greater

Table 6. Effect of the methanol-to-oil molar ratio on biodiesel yield

Test number	Molecular weight of methanol	Molecular weight of oil	Oil (g)	Oil (mol)	Methanol/oil molar ratio	Methanol (mol)	Methanol (g)	Yield (%)	Selected (✓)
1	32	876	14	0/016	8	0/1278	4	%37	
2	32	876	14	0/016	10	0/1598	5	%43	
3	32	876	14	0/016	12	0/1918	6	%53	✓
4	32	876	14	0/016	14	0/2237	7	%49	

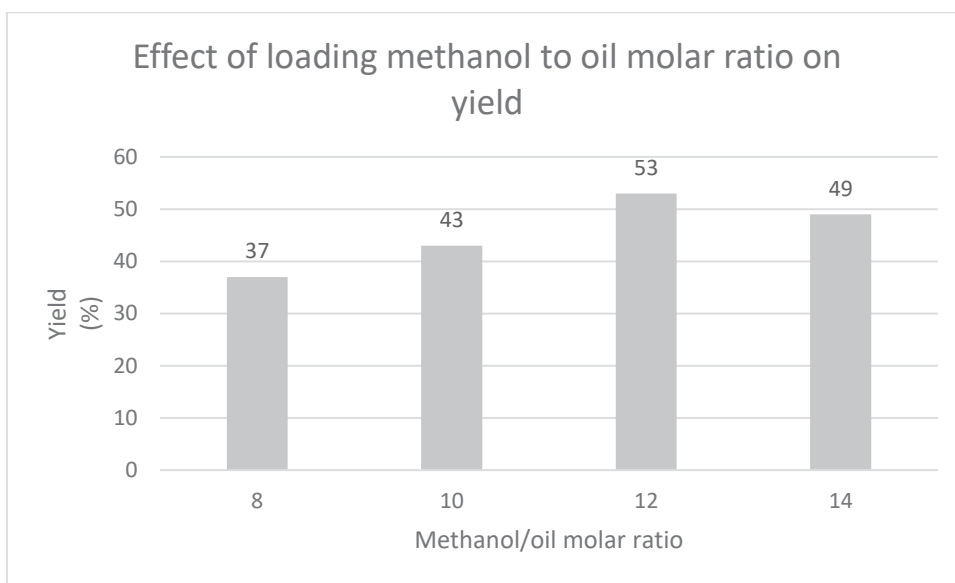


Figure 6. Effect of methanol to oil molar ratio on efficiency at 60°C and catalyst to oil ratio of 0.07 wt%

complexity in separating glycerol from the biodiesel phase due to high methanol concentrations ([18],[24]).

Hence, a molar ratio of 12:1 was chosen as the optimum value, optimizing yield and separation efficiency.

3.3.2. Effect of Reaction Temperature

The reaction temperature has a direct influence on the rate and equilibrium of the transesterification reaction. Experiments were performed at

50 °C, 60 °C, and 70 °C at the optimum molar ratio of 12:1. The findings are summarized in Table 7.

As seen in Table 6 and Figure 7, biodiesel yield was maximized at 60 °C, as anticipated based on the established optimum ranges for methanol-based transesterification. While increased reaction kinetics are the product of increased temperature, temperatures higher than 60–65 °C cause methanol evaporation due to its low boiling point of methanol, decreasing the effective reactant concentration and reaction efficacy ([25],[26]). 60 °C was thus adopted as the best reaction temperature for the process.

Table 7. Effect of reaction temperature on biodiesel yield

Test number	Oil (g)	Methanol/oil molar ratio	Methanol (g)	Temperature (°C)	Yield (%)	Selected (✓)
1	14	12	6	50	%45	
2	14	12	6	60	%53	✓
3	14	12	6	70	%47	

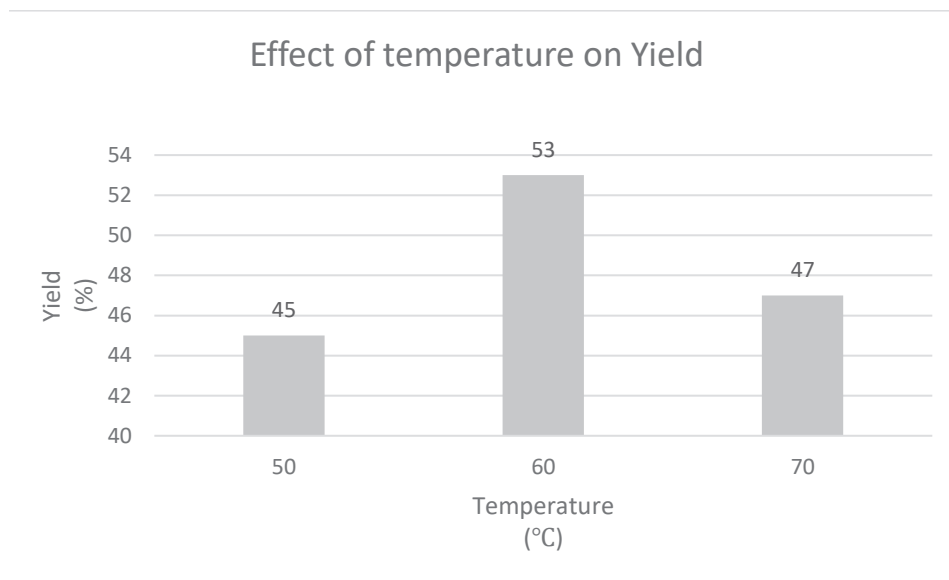


Figure 3. Effect of the temperature on yield with a methanol to oil molar ratio of 12:1 and a catalyst to oil ratio of 0.07 wt%

3.3.3. Catalyst Concentration Effect

The impact of catalyst loading was studied by varying the weight percentage of $\alpha\text{-Fe}_2\text{O}_3/\text{SiO}_2$ relative to oil (0.05 wt%, 0.07 wt%, and 0.10 wt%). Results are reported in Table 8.

Figure 8 and Table 7 show that the optimum amount of catalyst loading was 0.07 wt%. Amounts

lower than this failed to provide sufficient active sites for complete conversion, while higher concentrations resulted in particle agglomeration, diffusion limitations and reduced catalytic activity [27].

Thus, 1 g of catalyst (0.07 wt%) was determined as the optimum amount for achieving high biodiesel yield without wasteful material usage.

Table 8. Effect of catalyst loading on biodiesel yield

Test number	Oil (g)	Oil (mol)	Methanol/oil molar ratio	Weight percentage of catalyst to oil	Catalyst (g)	Yield (%)	Selected (✓)
1	14	0/016	12	0/05	0/7	%38	
2	14	0/016	12	0/07	1	%53	✓
3	14	0/016	12	0/01	1/4	%47	

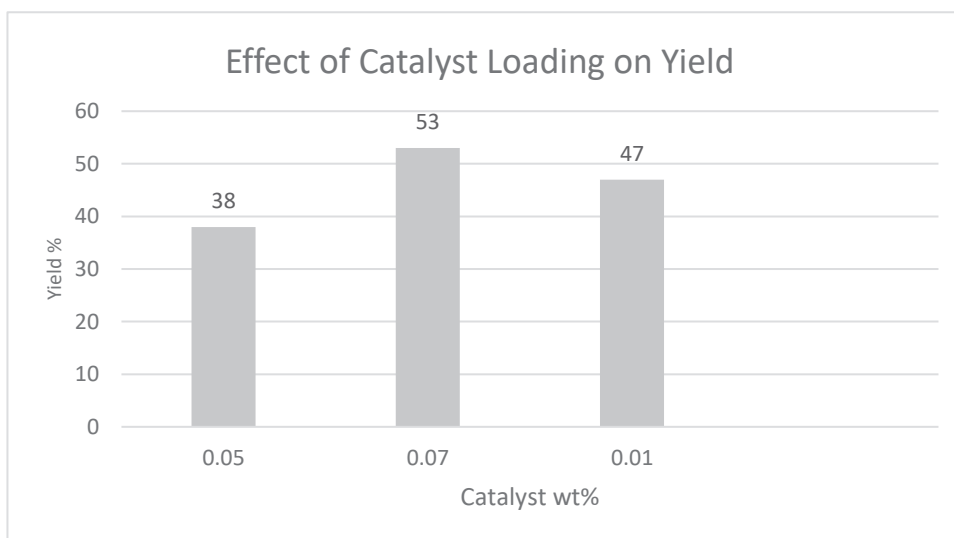


Figure 4. Effect of catalyst to oil weight percentage on yield at 60°C and methanol to oil molar ratio of 12:1

3.3.4. Fourier-Transform Infrared (FTIR) Analysis of Produced Biodiesel

FTIR spectroscopy was employed to confirm the chemical makeup of the biodiesel obtained from the $\alpha\text{-Fe}_2\text{O}_3/\text{SiO}_2$ catalyst. The resulting spectrum showed typical peaks of fatty acid methyl esters (FAMES), the main constituents of biodiesel indicating effective transesterification.

The notable absorption bands observed in the FTIR spectrum were:

1747 cm^{-1} : Strong peak for C=O stretching vibration of ester carbonyl groups, a clear indication of the presence of methyl esters.

2923 cm^{-1} and 2855 cm^{-1} : Refer to the asymmetric and symmetric stretching vibrations of $\text{-CH}_2\text{-}$ groups which are characteristic of the long

hydrocarbon chains.

1463 cm^{-1} and 1378 cm^{-1} : Mark the bending vibrations of $-\text{CH}_2$ and $-\text{CH}_3$ groups of saturated aliphatic compounds.

1238 cm^{-1} and 1163 cm^{-1} : Relevant to C–O stretching vibrations in ester functional groups.

3009 cm^{-1} : Small but characteristic peak due to =C–H stretching, which indicates the presence of some of the fatty acid chains as being unsaturated [28].

581 cm^{-1} and 460 cm^{-1} : Low-frequency peaks attributed to bending or lattice vibrations of the silica and iron oxide phases present in the catalyst matrix [29].

These results confirm the effective triglyceride to methyl ester conversion and reveal the catalytic activity of the $\alpha\text{-Fe}_2\text{O}_3/\text{SiO}_2$ system. The indication of both unsaturated and saturated ester groups on the IR spectrum establishes a diverse FAME composition, as expected for biodiesel from sunflower oil.

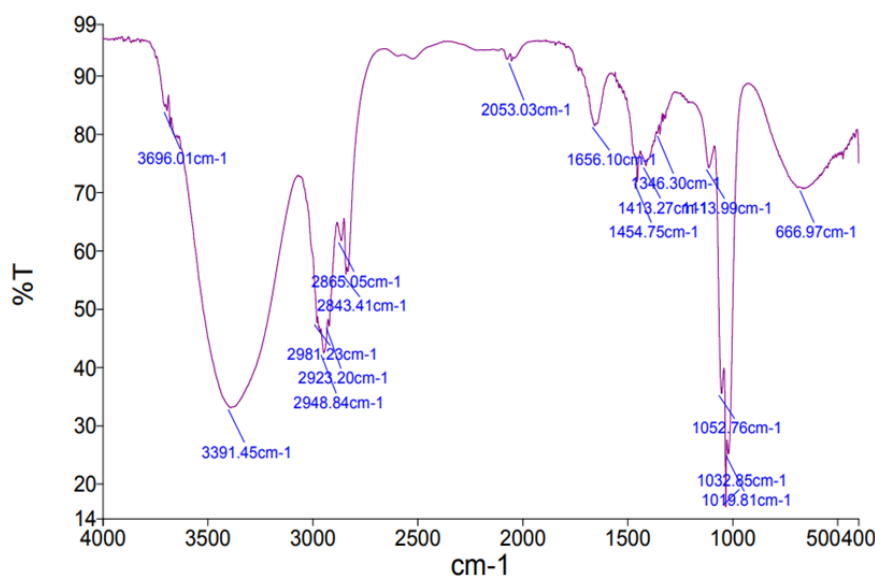


Figure 5. FTIR spectrum of produced biodiesel

3.3.5. Comparison of Catalysts and Yield Assessment

However, the highest biodiesel yield achieved in this study (53%) is slightly lower than those reported by some researchers with homogeneous catalysts as NaOH, KOH and nanostructured ones as $\text{CaO@Fe}_2\text{O}_3$ and HPA@ZrO_2 . This performance discrepancy can be primarily attributed to several technical and scientific factors. In case of the heterogeneous catalyst $\alpha\text{-Fe}_2\text{O}_3/\text{SiO}_2$, the interface between oil and methanol, interfacial contact, is limited, and therefore mass transfer and reaction kinetics are slower. Furthermore, partial evaporation of methanol at high temperature would lower

the actual molar ratio of methanol to oil, shifting the transesterification equilibrium backwards. Other issues, such as particle agglomeration, sintering, and surface clogging with organic intermediates can also reduce the total number of active catalytically sites.

In comparison, the solubility of NaOH or KOH in the reaction phase allows for better stoichiometric access is often better using homogeneous catalysts than that with solid bases, and results in higher yields under laboratory conditions. However, those catalysts typically need a long process to be neutralized, washed, and recovered which increases the post-reaction purification cost.

The $\alpha\text{-Fe}_2\text{O}_3/\text{SiO}_2$ catalyst has important in-

dustrial and environmentally friendly implications despite its moderate yield. It is prepared from inexpensive starting materials (industrial iron waste and synthetic silica), is thermally stable, non-toxic, and reusable. Unlike homogeneous system, it can be easily separated from the reaction solution and produces non-toxic waste. Their structural characteristics from hematite and silica phases are kinetically robust for chemical cycling reactions and show high promise for scalable industrial applications.

In conclusion, while the product yield in this study did not achieve the maximum reported yield, the economic, environmental, and operational advantages of $\alpha\text{-Fe}_2\text{O}_3/\text{SiO}_2$ make $\alpha\text{-Fe}_2\text{O}_3/\text{SiO}_2$ an attractive material for the sustainable development of biofuel production.

3.3.6. Catalyst Reusability and Structural Stability

A recycle test under the optimal reaction conditions was used to study the structural integrity and operational stability of the heterogeneous $\alpha\text{-Fe}_2\text{O}_3/\text{SiO}_2$ catalyst over three sequential rounds of the transesterification. The catalyst was separated from the reaction solution by centrifuge af-

ter each run, then washed with copious amount of methanol and distilled water, followed by drying at 100 °C, without further regeneration treatment. The percentage of the biodiesel yield in first, second, and third cycles were found to be 53, 45, and 39%, respectively.

This cycle-dependent decrease in yield results from the simultaneous deactivation of several factors such as the decrease in the number of active surface sites through particle agglomeration, mild thermal sintering during the reaction, and the poisoning of the surface by non-reacted organics intermediates. Furthermore, because of the repeated exposures to alcohol and reaction media, the microstructure of the silica support may also change, leading to activity loss.

Compared to that, 53% in the 1st cycle and 39% in the 3rd cycle activity could be recovered and reused, indicating good resistance to thermal treatment, integrity of structure and good recyclability under working conditions of the $\alpha\text{-Fe}_2\text{O}_3/\text{SiO}_2$ catalyst in the case of the present study. Its durability, efficiency, and stability indicate that the prepared catalyst can be a promising one for the biodiesel fabrication in industry.

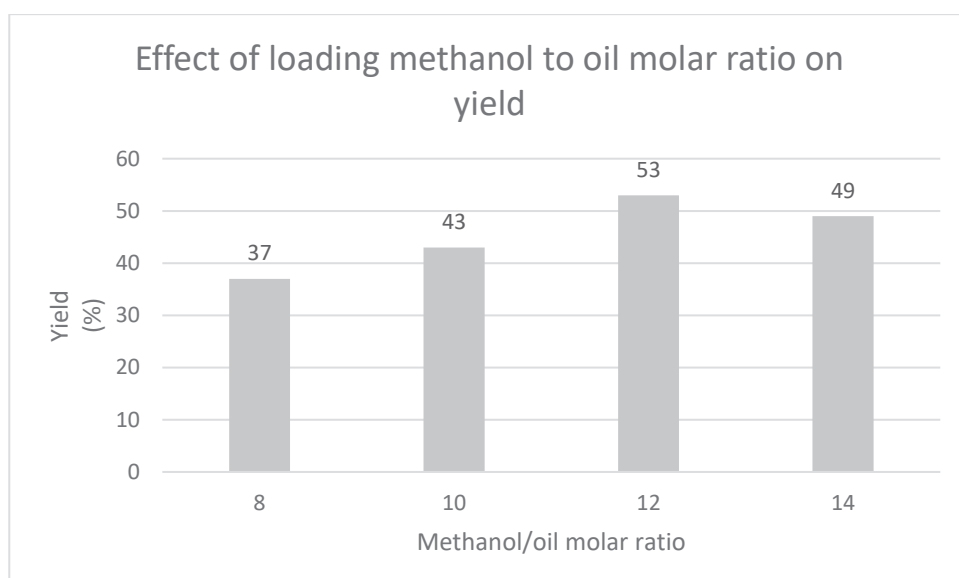


Figure 6. Biodiesel yield (%) over three consecutive reuse cycles of the $\alpha\text{-Fe}_2\text{O}_3/\text{SiO}_2$ catalyst under optimized transesterification conditions

3.3.7. Process Limitations and Operational Recommendations

The results of the synthesis and use of the heterogeneous $\alpha\text{-Fe}_2\text{O}_3/\text{SiO}_2$ catalyst in the production of biodiesel from edible oil were satisfactory; however, during the application, several technical limitations were identified which can be considered as the constraints of the study. A high content of iron waste in the early synthesis resulted in the formation of significantly larger and more densely packed nanoparticles, which could eventually impede the separation of the biodiesel and glycerol, as well as the entire product was colored orange, most likely due to partial dissolution or leaching from the catalyst crystal lattice of the catalyst in the reaction medium. Meanwhile, diluting sulphuric acid as a dangerous critical reaction, required precise control of safe conditions and temperature in addition to adding speed to avoid explosions and heat excess. Under some operating conditions, the adhesion and aggregation of iron particles were observed (especially at the higher temperatures or lower stirring speeds) which led to a decrease in the amount of the surface activated sites and a reduction in the extent of the reaction. Too high reaction temperature also caused the evaporation of methanol, lowered its effective molar quantity with oil, and thus shifting the transesterification equilibrium and resulting in a lower yield.

Future research should be oriented towards proper setup of the process that ensures systematic control and optimization of key parameters such as material weight ratio, stirring velocity and temperature along with reaction time using Design of Experiments (DoE). The modification of the surface of the catalyst and the employment of more stable supports can improve the stability of the activity during the successive cycles. Further, while centrifugation was used in this work for the phase separation, the optimization of its operational conditions may enhance the separation efficiency even in the presence of stable emulsions. These corrective actions may also favor repeatability, process safety, and industrial scale up.

4. Conclusion

In the present study, a highly active heterogeneous $\alpha\text{-Fe}_2\text{O}_3/\text{SiO}_2$ catalyst was synthesized from industrial waste iron and utilized for the transesterification of sunflower oil purified to biodiesel. The synthesis involved the dissolution of iron in 40% sulfuric acid, deposition on silica support, and thermal treatment under the best thermal conditions. Structural characteristics by XRD and FTIR established the development of crystalline hematite ($\alpha\text{-Fe}_2\text{O}_3$) thoroughly stabilized on the silica matrix, exhibiting good surface functionality and high-phase purity.

The catalytic performance of the synthesized nanocomposite was evaluated by monitoring essential reaction conditions. Optimum conditions were a molar ratio of methanol to oil of 12:1, catalyst loading of 0.07 wt%, temperature of 60 °C, and time of 6 hours. A biodiesel yield of up to 53% was achieved under these conditions.

FTIR spectrum of the final biodiesel product confirmed the presence of methyl ester functional groups, while physical property measurements (density (0.73 g/cm³) and kinematic viscosity (4.3 mm²/s)) were within the acceptable range for biodiesel standards. Gas chromatography further verified the composition and purity of the resulting biodiesel.

This research demonstrates that the industrial waste iron can be efficiently converted into an effective catalyst for renewable fuel production. The demonstrated pathway is cost-effective, environmentally friendly and scalable with a green approach to both biodiesel production and industrial waste valorization. Optimizing yield through catalyst development and system verification with alternative feedstocks such as waste cooking oils or non-food oils could be the focus of future work.

Since refined edible oil was used as the feedstock in this study, it would prove beneficial if alternative sources such as non-edible oils (e.g., castor or jatropha) and waste cooking oils be stud-

ies in future investigations. These feedstocks are attractive sources both economically and environmentally, because they are low-cost, abundant materials that can contribute to the environmental pollution problem. However, the polar compounds, high FFA content, and organic impurities in such oils demand that stability and performance of the α -Fe₂O₃/SiO₂ catalyst are re-enforced under these harsher conditions.

References

1. Vignesh, P., et al., *A review of conventional and renewable biodiesel production*. Chinese journal of chemical engineering, 2021. **40**: p. 1-17.
2. Bakhtawar, J., et al., *Trends in Biodiesel Production from Algae and Animal Fat Wastes: Challenges and Prospects*. Food Waste to Green Fuel: Trend & Development, 2022: p. 255-278.
3. Jjagwe, J., P.W. Olupot, and S. Carrara, *Iron oxide nanoparticles/nanocomposites derived from steel and iron wastes for water treatment: A review*. Journal of Environmental Management, 2023. **343**: p. 118236.
4. Fontes, W.C., et al., *Assessment of the use potential of iron ore tailings in the manufacture of ceramic tiles: From tailings-dams to "brown porcelain"*. Construction and Building Materials, 2019. **206**: p. 111-121.
5. Balasubramaniam, B., et al., *Iron oxides and their prospects for biomedical applications*, in *Metal Oxides for Biomedical and Biosensor Applications*. 2022, Elsevier. p. 503-524.
6. Qin, Q., X. Zhu, and X. Zhang, *Synthesis of α -Fe₂O₃ hollow spheres with rapid response and excellent selectivity towards acetone*. Materials Science and Engineering: B, 2022. **275**: p. 115482.
7. Kongsat, P., et al., *Synthesis of structure-controlled hematite nanoparticles by a surfactant-assisted hydrothermal method and property analysis*. Journal of Physics and Chemistry of Solids, 2021. **148**: p. 109685.
8. El-Bayoumy, F.I., et al., *Utilization of iron fillings solid waste for optimum biodiesel production*. Frontiers in Chemistry, 2024. **12**: p. 1404107.
9. Vilas Bôas, R.N. and M.F. Mendes, *A review of biodiesel production from non-edible raw materials using the transesterification process with a focus on influence of feedstock composition and free fatty acids*. Journal of the Chilean Chemical Society, 2022. **67**(1): p. 5433-5444.
10. Devianin, S., et al. *Vegetable oils as effective additives and replacements of diesel fuel in agriculture machinery engines*. in *IOP Conference Series: Earth and Environmental Science*. 2022. IOP Publishing.
11. Amirthavalli, V., A.R. Warriar, and B. Gurunathan, *Various methods of biodiesel production and types of catalysts*, in *Biofuels and bioenergy*. 2022, Elsevier. p. 111-132.
12. Cullen, A., D.W. Johnson, and I.A. York, *Catalyst and a process for the production of ethylenically unsaturated carboxylic acids or esters*. 2023, Google Patents.
13. Ursachi, I., A. Stancu, and A. Vasile, *Magnetic α -Fe₂O₃/MCM-41 nanocomposites: Preparation, characterization, and catalytic activity for methylene blue degradation*. 2012.
14. Rahimi, T., et al., *Catalytic performance of MgO/Fe₂O₃-SiO₂ core-shell magnetic nanocatalyst for biodiesel production of Camelina sativa seed oil: Optimization by RSM-CCD method*. Industrial Crops and Products, 2021. **159**: p. 113065.
15. Ziyadi, H., M. Baghali, and A. Heydari, *The synthesis and characterization of Fe₂O₃@ SiO₂-SO₃H nanofibers as a novel magnetic core-shell catalyst for formamidine and formamide synthesis*. Heliyon, 2021. **7**(6).
16. Teo, S.H., et al., *Efficient biodiesel production from Jatropha curcus using CaSO₄/Fe₂O₃-SiO₂ core-shell magnetic nanoparticles*. Journal of cleaner production, 2019. **208**: p. 816-826.

17. Hanif, M., et al., *Nano-Magnetic CaO/Fe₂O₃/feldspar catalysts for the production of biodiesel from waste oils*. *Catalysts*, 2023. **13**(6): p. 998.
18. Erchamo, Y.S., et al., *Improved biodiesel production from waste cooking oil with mixed methanol–ethanol using enhanced eggshell-derived CaO nano-catalyst*. *Scientific Reports*, 2021. **11**(1): p. 6708.
19. Mohan, S. and P. Dinesha, *Emulsification of waste cooking oil biodiesel blend with hydrogen peroxide to assess tailpipe emissions and performance of a compression ignition engine*. *Heat Transfer*, 2022. **51**(4): p. 3721-3735.
20. Ajala, E.O., et al., *Synthesis of solid catalyst from dolomite for biodiesel production using palm kernel oil in an optimization process by definitive screening design*. *Brazilian Journal of Chemical Engineering*, 2019. **36**(2): p. 979-994.
21. Xia, S., et al., *Sustainable biodiesel production via transesterification of vegetable oils and waste frying oil over reusable magnetic Ca₂Fe₂O₅/CaO@ MgFe₂O₄-Fe₂O₃ catalyst*. *Energy Sources, Part A: Recovery, Utilization, and Environmental Effects*, 2023. **45**(3): p. 8047-8061.
22. Shaker, M. and D. Elhamifar, *Sulfonic acid supported on magnetic methylene-based organosilica as an efficient and recyclable nanocatalyst for biodiesel production via esterification*. *Frontiers in Energy Research*, 2020. **8**: p. 78.
23. Osman, A.I., et al., *Optimizing biodiesel production from waste with computational chemistry, machine learning and policy insights: a review*. *Environmental Chemistry Letters*, 2024. **22**(3): p. 1005-1071.
24. Tsaoulidis, D., E. Garciadiego-Ortega, and P. Angeli, *Intensified biodiesel production from waste cooking oil and flow pattern evolution in small-scale reactors*. *Frontiers in Chemical Engineering*, 2023. **5**: p. 1144009.
25. Buchori, L., et al., *Effect of temperature and concentration of zeolite catalysts from geothermal solid waste in biodiesel production from used cooking oil by esterification–transesterification process*. *Processes*, 2020. **8**(12): p. 1629.
26. Zhang, Q., et al., *Immobilizing Ni (II)-exchanged heteropolyacids on silica as catalysts for acid-catalyzed esterification reactions*. *Periodica Polytechnica Chemical Engineering*, 2021. **65**(1): p. 21-27.
27. Emberru, R.E., et al., *A review of catalyst modification and process factors in the production of light olefins from direct crude oil catalytic cracking*. *Sci*, 2024. **6**(1): p. 11.
28. Mahamuni, N.N. and Y.G. Adewuyi, *Fourier transform infrared spectroscopy (FTIR) method to monitor soy biodiesel and soybean oil in transesterification reactions, petrodiesel– biodiesel blends, and blend adulteration with soy oil*. *Energy & Fuels*, 2009. **23**(7): p. 3773-3782.
29. Hossain, M.S. and S. Ahmed, *FTIR spectrum analysis to predict the crystalline and amorphous phases of hydroxyapatite: a comparison of vibrational motion to reflection*. *RSC advances*, 2023. **13**(21): p. 14625-14630.

تولید پایدار بیودیزل از روغن خوراکی از طریق ترانس استریفیکاسیون با کاتالیست ناهمگن آهن پایه بازیافتی $\alpha\text{-Fe}_2\text{O}_3/\text{SiO}_2$: مطالعات عملکرد و قابلیت استفاده مجدد

فائزه مسلمان زاده، تارا غفاری نژاد، رامین کریم زاده*

ایران، تهران، دانشگاه تربیت مدرس، دانشکده مهندسی شیمی، صندوق پستی ۸۳۸-۱۴۱۵۵

مشخصات مقاله

تاریخچه مقاله:

دریافت ۷ مرداد ۱۴۰۴

دریافت پس از اصلاح ۱۸ شهریور

۱۴۰۴

پذیرش نهایی ۲۳ آذر ۱۴۰۴

کلمات کلیدی:

ضایعات آهن، کاتالیست

ناهمگن، $\alpha\text{-Fe}_2\text{O}_3/\text{SiO}_2$

ترانس استریفیکاسیون،

بیودیزل، فعال سازی حرارتی،

انرژی تجدیدپذیر.

*عهده دار مکاتبات:

رایانامه: ramin@modares.ac.ir

تلفن:

نحوه استناد به این مقاله:

Mosalmanzadeh F, Ghaffarinejad T, Karimzadeh R, Sustainable Biodiesel Production from Edible Oil through Transesterification with Waste Iron-Based $\alpha\text{-Fe}_2\text{O}_3/\text{SiO}_2$ Heterogeneous Catalyst: Performance and Reusability Studies, Journal of Oil, Gas and Petrochemical Technology, 2025; 12(2): 81-96. DOI:10.22034/jogpt.2026.537855.1142.



This work is licensed under the Creative Commons Attribution 4.0 International License.

To view a copy of this license, visit <http://creativecommons.org/licenses/by/4.0/>.